Resonance production in double gap events and exclusive four pion photoproduction in ultra-peripheral Pb-Pb collisions at $\sqrt{s_{NN}} = 5.02$ TeV in ALICE

Rainer Schicker, Phys. Inst., Heidelberg
(on behalf of ALICE Collaboration)

Int. Workshop on Partial Wave Analyses (PWA13/ATHOS8)
May 28 - June 1, 2024

UNIVERSITÄT HEIDELBERG
ZUKUNFT SEIT 1386

ALICE

BMBF Forschungsschwerpunkt
ALICE Experiment 202
ALICE

The ALICE upgrade in long shutdown LS2 2019-2022

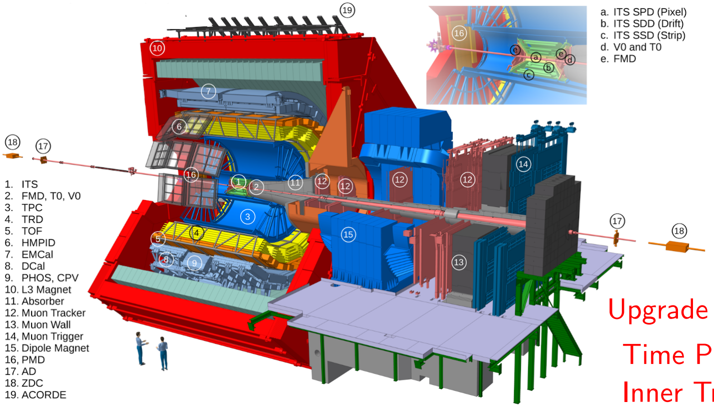

Upgrade of:

- Time Projection Chamber (TPC)
- Inner Tracking System (ITS)
- Fast Interaction Trigger (FIT)
- Computing system On-Offline (O^2)

midrapidity tracks in central barrel:

ITS,TPC,TRD,TOF: $-0.9 < \eta < 0.9$

The TPC

- Total length 5m,
  radial dimension 83.5 cm $< r <$ 254.5 cm
- Gas mixture Ne-CO_2-N_2 (90-10-5)
- Central electrode and field cage,
  uniform E-field 400 V/cm along beam-axis
- Charged particles traversing TPC volume ionise the gas atoms
- Ionisation electrons drift to endplates,
  segmented readout, $\sim$ 550000 pads
- 3-d measurement of ionisation clusters,
  x and y-coordinate from pad position,
  z-coordinate from drift time

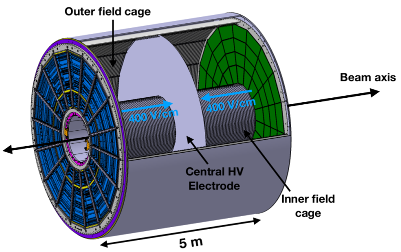

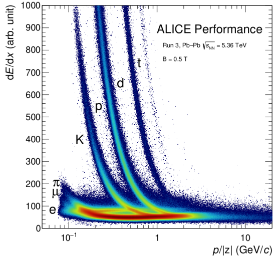

The TPC upgrade

- Positive-ion backflow a major issue in TPC running conditions
- Positive-ion backflow usually controlled by gating grid in Runs 1,2, rate limit $\sim$ 3 kHz
- Electron multiplication in Run 3 by staging of 4 Gas Electron Multiplier (GEM) foils
- Ion backflow $\leq$ 0.7% with 4 staged GEMs
- Pb-Pb data taking rate increased from 1 kHz in Runs 1,2 to 50 kHz in Run 3
- 3-d cluster position information is input for global track reconstruction
- still significant space charge distortions calibrated continuously

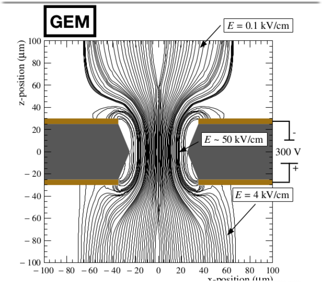

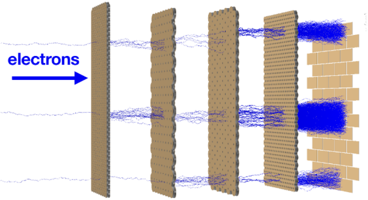

The ITS upgrade

- A new ITS detector: *improved resolution, less material, faster readout*

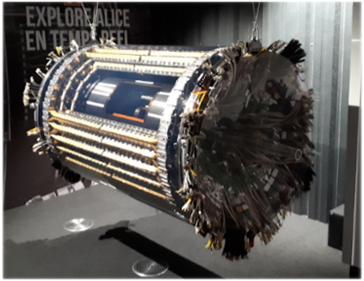

ITS Run 1,2 → ITS Run 3

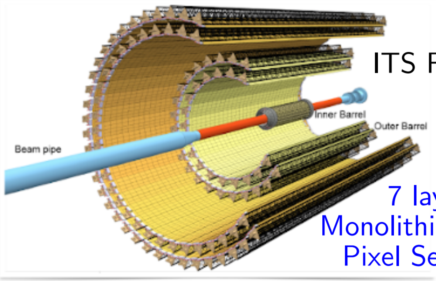

7 layers of Monolithic Active Pixel Sensors

	ITS Run 1,2	ITS Run 3
Distance to IP (mm)	39	22
X_0 (innermost layer) (%)	$\sim$1.14	$\sim$0.35
Pixel pitch (μm^2)	50 x 425	27 x 29
Readout rate (kHz)	1	100
Spatial resolution ($r\varphi$ x z) (μm^2)	11 x 100	5 x 5

The FIT upgrade

- The Fast Interaction Trigger (FIT) detector serves as interaction trigger, online luminometer, and forward multiplicity counter
- Provides precise collision time for time-of-flight based particle identification

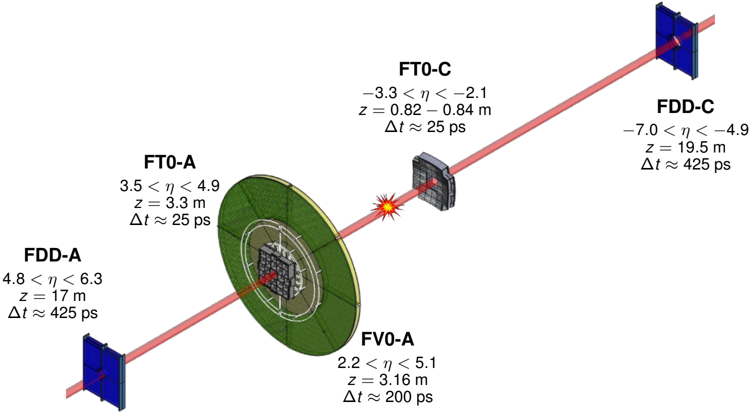

The computing system upgrade

- New common Online-Offline (O^2) computing system

3.6 TeraBytes/s raw data
$\rightarrow$ up to 170 GBytes/s to disk

50k CPUs
2700 GPUs
130 PetaBytes disk

Data statistics in Run 2 and Run 3

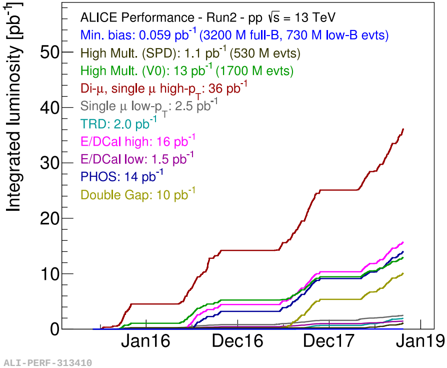

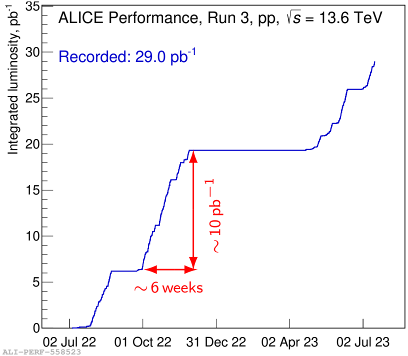

Double gap data sample of 10 pb^{-1} in Run 2

Central barrel data sample of ∼10 pb^{-1} per 6 weeks of data taking in 2022,2023

Central diffractive production at the LHC

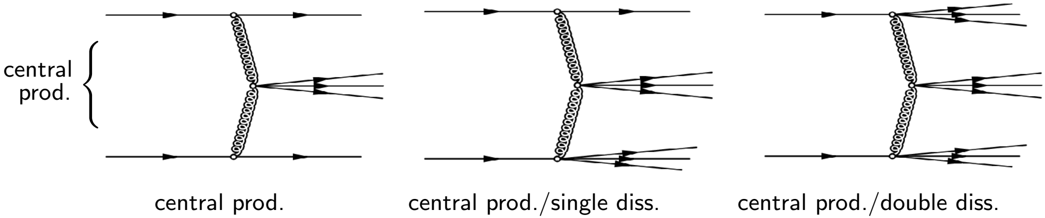

- Pomerons $\mathbb{P}$ and Reggeons $\mathbb{R}$ contribute to these topologies
- Rapidity gaps can also be due to photon and $W^{\pm}$,Z-exchange
- Pomerons and photons contribute differently in pp, pA and AA

Experimental identification of these topologies by

1. Tag the foward protons or fragments by Roman pots (no Roman Pots in ALICE)
2. Define rapidity range on both sides of midrapidity void of activity (rapidity gap)
   $\rightarrow$ no signal in FIT detector $\rightarrow$ double gap event

Pion pairs in double gap events

- particle ident. by dE/dx from TPC, identify pion pairs $\pi^+\pi^-, \pi^+\pi^+, \pi^-\pi^-$

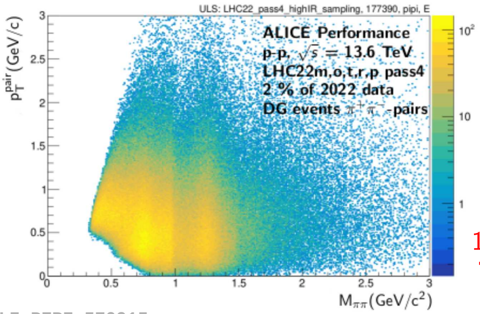

$\pi^+\pi^-$-pairs

1-d proj.

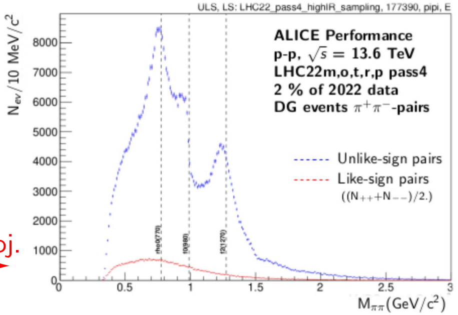

$\pi^+\pi^-, \pi^+\pi^+, \pi^-\pi^-$-pairs

- resonance structures seen in the pion sector: $\rho(770)$, $f_0(980)$, $f_2(1270)$

Kaon pairs in double gap events

- particle ident. by dE/dx from TPC, identify kaon pairs K^+K^-, K^+K^+, K^-K^-

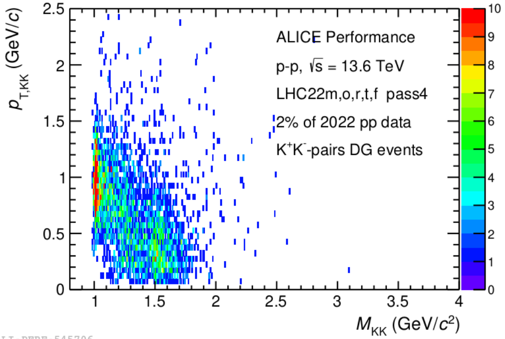

K^+K^--pairs

1-d proj.

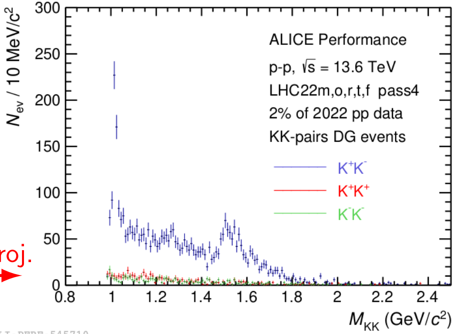

K^+K^-, K^+K^+, K^-K^--pairs

- resonance structures seen in the kaon sector: $\phi(1020)$, $f_2(1270)$, $f_2'(1525)$

A model of $q\bar{q}$ bound states

- *"Mesons in a relativized quark model with chromodynamics"*
  S. Godfrey, N. Isgur, Phys.Rev. D 32 (1985) 189.
- Calculate $q\bar{q}$ bound states in a relativistic potential V(p, r)

$$V(\mathrm{p},\mathrm{r}) = H^{conf} + H^{so} + H^{hyp} + H_A \quad (1)$$

H^{conf}: confining pot., H^{so}: spin-orbit inter., H^{hyp}: hyperfine inter., H_A: annihilation inter.

isoscalar meson sector: - states with predominant light quark (u,d) composition
- states with predominant strange quark (s) composition

isoscalars with (hidden) strangeness

spectroscopic notation $n\,^{2S+1}L_J$:

- n radial quantum number
- S spin
- L orbital angular momentum
- J total angular momentum

$n\,^{2S+1}L_J$	mass sol.(1)	PDG	J^{PC}	mass (PDG)	width (PDG)
1^3S_1	1020	ϕ	1^{--}	1019	4
1^3P_2	1530	f_2'	2^{++}	1518	86
1^3D_3	1900	ϕ_3	3^{--}	1854	87
1^3F_4	2200				

mass and width in (MeV)

Nonlinear, complex meson trajectories

- Complex Regge trajectory based on Dual Amplitude with Mandelstam Analyticity (DAMA)
- Real and imaginary part of trajectory are connected by dispersion relation

$$\Re e\,\alpha(s) = \alpha(0) + \frac{s}{\pi} PV \int_0^\infty ds' \frac{\Im m\,\alpha(s')}{s'(s'-s)}. \tag{2}$$

- Imaginary part is related to the decay width

$$\Gamma(M_R) = \frac{\Im m\,\alpha(M_R^2)}{\alpha'\, M_R}. \tag{3}$$

- Imaginary part chosen as sum of single threshold terms

$$\Im m\,\alpha(s) = \sum_n c_n (s - s_n)^{1/2} \left(\frac{s - s_n}{s}\right)^{|\Re e\,\alpha(s_n)|} \theta(s - s_n). \tag{4}$$

- Imag. part of trajectory in Eq.(4) has correct threshold and asymptotic behaviour
- The c_n are expansion coefficients, s_n are threshold energies of decay channels

Reggeizing isoscalar states with hidden strangeness

- DAMA fit to the isoscalar strangeness states $\phi, f_2^{'}, \phi_3$ defines the $(\phi, f_2^{'})$-trajectory

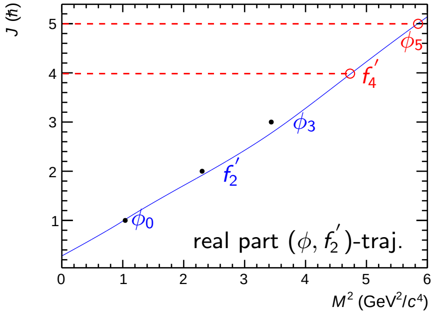

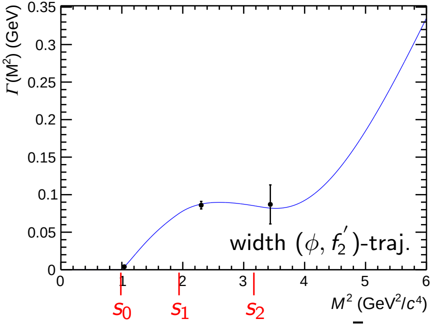

- DAMA fit of $(\phi, f_2^{'})$-trajectory predicts
  - $f_4^{'}$ state, mass 2182 MeV and width 156 MeV
  - ϕ_5 state, mass 2417 MeV and width 310 MeV

$\phi_3 \to K^* \bar{K}^*,\ s_2 = 3.18$ GeV^2

$f_2^{'} \to K K^*, s_1 = 1.92$ GeV^2

$\phi \to K \bar{K}, s_0 = 0.97$ GeV^2

Four pion production in ultra-peripheral Pb-Pb collisions

- Nuclei at ultra-relativistic energies carry strong electromagnetic fields
- These electromagnetic fields define a flux of quasi-real photons (Weizsäcker-Williams)

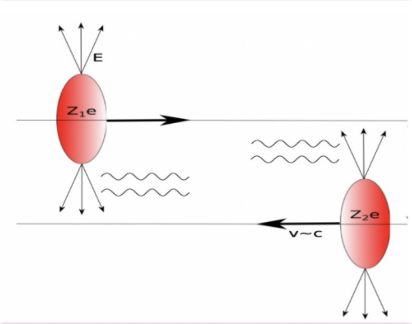

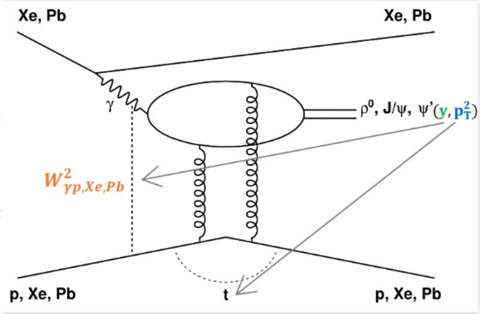

Coherent production of $\rho^0(770)$ in Pb-Pb and Xe-Xe collisions

- Production of ρ^0 has been studied at HERA by H1 and ZEUS, and at the LHC by CMS in ultra-peripheral pA collisions

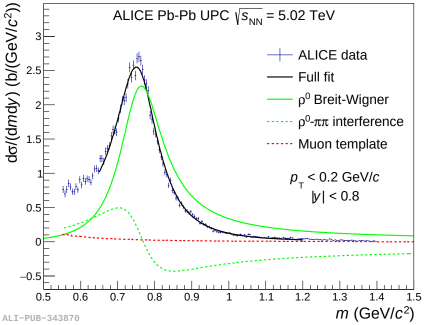

ALICE Coll., Coherent photoproduction of ρ^0 vector mesons in ultra-peripheral Pb-Pb collisions at $\sqrt{s_{NN}} = 5.02$ TeV, **JHEP 06 (2020) 035**

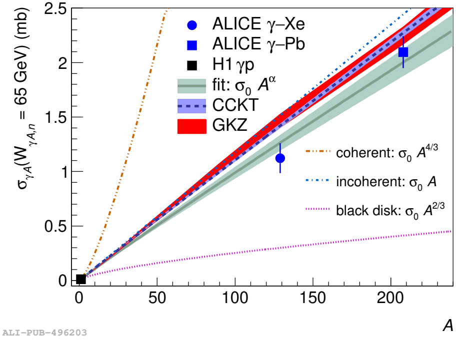

ALICE Coll., First measurement of coherent ρ^0 photoproduction in ultra-peripheral Xe-Xe collisions at $\sqrt{s_{NN}} = 5.44$ TeV, **Phys. Lett. B 820 (2021) 136481**

Photoproduction of excited ρ states

- $\rho^0(770)$ photoproduction has been studied
  - in ep collisions by H1 and ZEUS
  - in Pb-Pb and Xe-Xe UPC collisions by ALICE
  - in Au-Au UPCs by STAR
  - in p-Pb UPCs by CMS
- Production of excited ρ states expected in UPCs
- Mass and width of these resonances listed by Particle Data Group
- Theory curve taken from M.Klusek-Gawenda and D.Tapia Takaki, Acta Phys. Polon. B51 (2020) 6, 1393

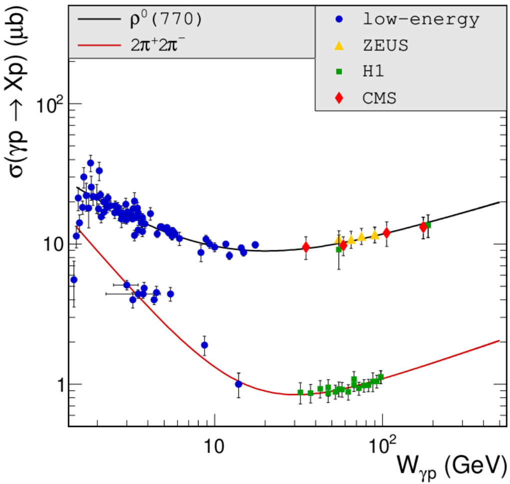

ALICE data four pion production

ALICE Coll., arXiv:2404.07542

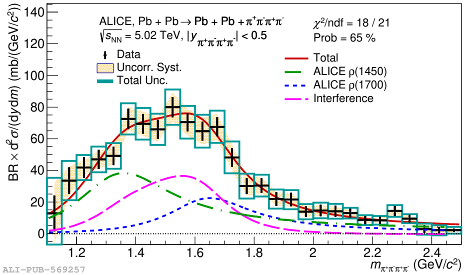

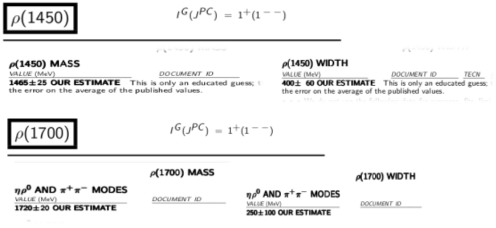

Four pion inv. mass spectrum fit:

$$\frac{d\sigma}{dm_{\pi\pi\pi\pi}} = \left|A \cdot BW_1 + e^{-i\phi} \cdot B \cdot BW_2\right|^2$$

Breit-Wigner fit values:

$M_1 = 1385 \pm 14$ (stat.) $\pm$ 36 (syst.) MeV
$\Gamma_1 = 431 \pm 36$ (stat.) $\pm$ 82 (syst.) MeV
$M_2 = 1663 \pm 13$ (stat.) $\pm$ 22 (syst.) MeV
$\Gamma_2 = 357 \pm 31$ (stat.) $\pm$ 49 (syst.) MeV

Breit-Wigner (BW) parametrisation of amplitude:

$$BW(m) = \frac{\sqrt{m_{res} \cdot m \cdot \Gamma}}{m^2 - m_{res}^2 + i \cdot m_{res} \cdot \Gamma}$$

Two resonance fit gives better result than single resonance fit: $\chi^2/\text{ndf} = 18/21$ vs $48/25$.

Mixing angle $\phi = 1.52 \pm 0.16(stat.) \pm 0.19(syst.)$

Conclusions and outlook

- ALICE is taking data in Run 3 after a major upgrade in long shutdown LS2
- First analysis of strangeness in double gap events in pp collisions shows clear evidence for strangeonia states $\phi(1020)$ and $f_2'(1525)$
- Improved particle identification by combining TPC dE/dx with TOF information
- 50 times larger data sample from data taking 2022/2023 available for analysis
- The search for the $f_4'(2182)$ and $\phi_5(2417)$ state
- Nature of the known $\phi(1680)$: radial excitation of the $\phi(1020)$?
  The $2^3S_1(1.69)$ state in Godfrey-Isgur model?
  Leading pole of a subleading isoscalar Regge trajectory in the strange sector?
- Extend strangeness analysis to $(u, d)\bar{s}$ kaonia and $(\bar{u}, \bar{d})s$ antikaonia states by analysing πK pairs
- First measurement of exclusive four pion photoproduction in ultra-peripheral Pb-Pb collisions at the LHC

BACKUP

Isoscalar states in light-quark and strangeness sector

- The Godfrey-Isgur model predicts isoscalar states in the light-quark and strangeness sector
- $\underline{1^3S_1}$, $J^{PC} = 1^{--}$:
  One state at 780 MeV, one state at 1020 MeV. The 780 MeV state is identified as $\omega(782)$(light-quark sector), the 1020 MeV as $\phi(1020)$ (strangeness sector).
- $\underline{1^3P_2}$, $J^{PC} = 2^{++}$:
  States at 1280 MeV and 1530 MeV. The 1280 MeV state is identified as $f_2(1270)$ (light-quark sector), Br($\pi\pi$) $\sim$ 85%, Br($K\bar{K}$) $\sim$ 5%, the 1530 MeV as $f_2^{'}(1525)$ (strangeness sector), Br($\pi\pi$) $\sim$ 1%, Br($K\bar{K}$) $\sim$ 88%.
- $\underline{1^3D_3}$, $J^{PC} = 3^{--}$:
  States at 1680 MeV and 1900 MeV. The 1680 MeV state is identified as $\omega_3(1670)$ (light-quark sector), no BR's, the 1900 MeV as $\phi_3(1850)$ (strangeness sector), no BR's.
- $\underline{1^3F_4}$, $J^{PC} = 4^{++}$:
  States at 2010 MeV and 2200 MeV. The 2010 MeV state is identified as $f_4(2050)$ (light-quark sector), Br($\pi\pi$) $\sim$ 17%, Br($K\bar{K}$) $\sim$ 0.7%. PDG lists only one F_4 state.

Space Charge Distortions

- Ions from the amplification stage move back into the drift volume
- Ions are slow (~200 ms for full drift)
  - Ions from large number of events pile up (~10k events @ 50 kHz IR)
  - Significant space-charge density (SCD) in drift volume
  - Large average distortions (O(5-10 cm))
  - Intrinsic TPC resolution: ~200 μm
  - $\rho_{SC} \sim I_{prim} \bullet gain \bullet IBF$
- Correction strategy based on reference tracks using ITS extrapolations.
- Corrections every few ms!
- Challenge for Run 3 with continuous readout

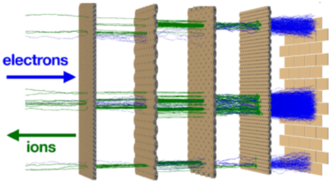

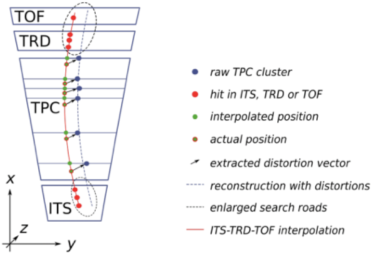

Space Charge Distortion Maps

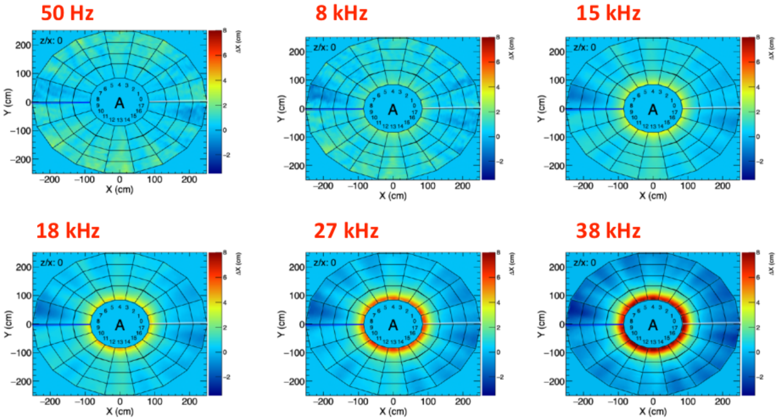

- Average maps. Fluctuations and IR dependence are treated on top.
- Distortions up to ~8 cm in radial direction!
- Corrections applied on the ms timescale to remove fluctuations.